



Published in final edited form as:

NeuroUrol Urodyn. 2020 January ; 39(1): 108–115. doi:10.1002/nau.24170.

Role of p38 MAP kinase signaling pathways in storage and voiding dysfunction in mice with spinal cord injury

Nobutaka Shimizu^{1,2}, Naoki Wada¹, Takahiro Shimizu¹, Takahisa Suzuki¹, Masahiro Kurobe¹, Anthony J. Kanai³, William C. de Groat⁴, Mamoru Hashimoto², Akihide Hirayama⁵, Hirotsugu Uemura², Naoki Yoshimura^{1,4}

¹Department of Urology, University of Pittsburgh, Pittsburgh, Pennsylvania

²Department of Urology, Faculty of Medicine, Kindai University, Osaka-Sayama, Japan

³Department of Medicine, University of Pittsburgh, Pittsburgh, Pennsylvania

⁴Department of Pharmacology and Chemical Biology, University of Pittsburgh, Pittsburgh, Pennsylvania

⁵Department of Urology, Faculty of Medicine, Kindai University Nara Hospital, Nara, Japan

Abstract

Aim: To investigate the role of p38 MAP kinase in lower urinary tract dysfunction in mice with spinal cord injury (SCI).

Methods: Cystometry and external urethral sphincter-electromyography were performed under an awake condition in 4-week SCI female mice. Two weeks after SCI, a catheter connected to an osmotic pump filled with a p38 mitogen-activated protein kinase (MAPK) inhibitor or artificial cerebrospinal fluid (CSF) was implanted into the intrathecal space of L6-S1 spinal cord for continuous intrathecal instillation at infusion rate of 0.51 $\mu\text{L}/\text{h}$ for 2 weeks before the urodynamic study. L6 dorsal root ganglia were then removed from CSF and p38 MAPK inhibitor-treated SCI mice as well as from CSF-treated normal (spinal intact) mice to evaluate the levels of transient receptor potential cation channel subfamily V member 1 (TRPV1), tumor necrosis factor- α (TNF- α), and inducible nitric oxide synthase (iNOS) transcripts by real-time polymerase chain reaction.

Results: In p38 MAPK inhibitor-treated SCI mice, nonvoiding contractions during bladder filling, bladder capacity, and post-void residual volume were significantly reduced while micturition pressure and voiding efficiency were significantly increased in comparison to these measurements in CSF-treated SCI mice. The expression of TRPV1, TNF- α , and iNOS messenger RNA was increased in SCI mice compared with expression in spinal intact mice and significantly decreased after p38 MAPK inhibitor treatment.

Conclusions: The p38 MAPK signaling pathway in bladder sensory neurons or in the spinal cord plays an important role in storage and voiding problems such as detrusor overactivity and inefficient voiding after SCI.

Keywords

detrusor overactivity; mice; p38 MAP kinase; spinal cord injury; urodynamics

1 | INTRODUCTION

Chronic spinal cord injury (SCI) rostral to the lumbosacral level induces detrusor overactivity (DO) during the storage phase, which is mediated by spinal reflexes triggered by hyperexcitable C-fiber afferent pathways. Also, during the voiding phase, inefficient voiding is commonly observed due to detrusor-sphincter dyssynergia (DSD) after SCI.¹ It has been shown that neurotrophic factors released within the urinary bladder or the spinal cord are important mediators inducing neurogenic lower urinary tract dysfunction (LUTD) after SCI.²

Previous research in rats and mice indicates that nerve growth factor (NGF) is overexpressed in the bladder and spinal cord following SCI and can induce changes in C-fiber bladder afferent pathways leading to the emergence of LUTD.³⁻⁵ It has been proposed that afferent nerves in the bladder take up NGF and transport it to the dorsal root ganglia (DRG), where it alters the expression of ion channels and receptors and induces hyperexcitability of C-fiber bladder afferent pathways, which in turn initiates neurogenic LUTD.^{1,6,7} Effects of NGF are known to be mediated by second messenger signaling pathways involving phosphorylation and stimulation of a serine-threonine kinase (p38 MAP kinase),⁸ which mediates cellular responses to a variety of chemical and physical insults.⁹ However, it remains to be elucidated whether the p38 mitogen-activated protein kinase (MAPK) pathway is also involved in LUTD induced by SCI although we previously reported the differences in urodynamic characteristics in normal and SCI mice.¹⁰ Therefore, in this study, we focused on the effects of a p38 MAPK inhibitor in SCI mice to clarify the role of the p38 MAPK pathway in SCI-induced storage and voiding dysfunction.

2 | MATERIALS AND METHODS

2.1 | Animal preparation

A total of 30, 9- to 10-week-old female C57BL/6N mice (Envigo, Frederick, MD) weighing between 18 and 22g were used. SCI mice underwent complete transection of the spinal cord at the thoracic 8/9 level under 1.5% to 2.0% isoflurane anesthesia according to methods described previously.¹⁰ To prevent urinary tract infection SCI animals were treated with ampicillin (100 mg/kg, subcutaneously) once daily for 5 days post-SCI followed by twice per week injections until final experiments. The bladders of SCI animals were emptied by manual bladder compression and perineal stimulation daily for 4 weeks post-SCI. Spinal intact (SI) mice underwent a sham operation without spinal cord transection, and received the antibiotic treatment with ampicillin once daily for 5 days after surgery.

Two weeks after SCI, an intrathecal catheter (Mouse Intrathecal Catheter; Alzet Osmotic Pumps, Cupertino, CA) connected to an osmotic pump (Alzet Osmotic Pumps) filled with SB203580 (1 mg/mL), a p38 MAPK inhibitor (EMD Millipore Corp, Billerica, MA) or

cerebrospinal fluid (CSF) (Tocris Bioscience, Bristol, UK) was implanted into the intrathecal space of L6-S1 spinal cord for continuous intrathecal instillation at infusion rate of 0.51 $\mu\text{L/h}$ for 2 weeks.

For cystometric analysis, mice were divided into two groups: (a) SCI treated with CSF ($n = 4$) and (b) SCI treated with p38 MAPK inhibitor ($n = 4$). In real-time polymerase chain reaction (PCR), L6 DRG were removed from CSF-treated SCI mice ($n = 8$) and p38 MAPK inhibitor-treated SCI mice ($n = 5$) as well as CSF-treated SI mice ($n = 6$). Mice were housed with four animals per cage according to the IACUC's recommendation for humane animal care, maintained in an air-conditioned room at 22°C to 24°C in a 12-12 hour light-dark cycle with lights on at 07:00 hour, and given food and water ad libitum.

2.2 | Cystometric analysis

Four weeks after SCI, cystometrograms (CMGs) were recorded under an awake condition. A lower midline abdominal incision was performed and a PE-50 tube (Clay-Adams, Parsippany, NJ) with the end flared by heat was inserted into the bladder from the bladder dome as a cystostomy catheter under 1.5% to 2.0% isoflurane anesthesia. The midline abdominal incision was then closed. Thereafter the animals were gently restrained in a cage (Economy holder 15–30 g; Torrington, CT) and the cystometry catheter was connected via a three-way stopcock to a pressure transducer and to a syringe pump. After the animals recovered from anesthesia, CMGs were recorded by filling the bladder with saline (0.01 mL/min) to observe rhythmic and stable bladder contractions for at least 180 minutes. Then, cystometric parameters were measured during a single voiding cycle; after the bladder was emptied, the infusion pump was turned on and the bladder allowed to fill until reflex voiding occurred. The nonvoiding contractions (NVCs) were defined as bladder pressure amplitude increases above 8 mm Hg.¹⁰ The number of NVCs was counted during the filling phase of at least two voiding cycles, and divided by minutes of the duration of filling in each mouse to obtain the average values for the statistical comparison among groups. We also measured maximal micturition pressure (MP) and postvoid residual urine (PVR) volume, which was determined by withdrawing intravesical fluid through the bladder catheter by gravity after voiding. Bladder capacity was calculated from the infusion rate (0.01 mL/min) multiplied by the time to void (minutes) after starting saline infusion. Voided volume (VV) was calculated by subtracting PVR from the calculated bladder capacity. We also calculated percent voiding efficiency ($\text{VV}/\text{bladder capacity} \times 100$). These parameters were evaluated in two serial CMGs by measuring PVR after each void, which were then averaged for statistical analyses (Figure 1).^{5,10}

2.3 | External urethral sphincter-electromyogram analysis

After cystometric analysis, external urethral sphincter (EUS)-electromyograms (EMGs) were recorded under an awake condition according to the methodology described in a previous paper.¹⁰ Animals were reanesthetized briefly for insertion of the EMG electrodes. Epoxy-coated stainless steel wire EMG electrodes (50 μm diameter; M. T. Giken, Tokyo, Japan) were placed percutaneously into the EUS. This was performed using a 28-gauge needle with a tip portion of EMG electrode hooked at the needle tip. The needle was inserted into the sphincter and then withdrawn to leave the EMG wires embedded in the muscle.

After every EUS-EMG experiment, the location of EMG wire ends were visually examined by dissecting each animal, and if they were located more than 1.0 mm from the urethra, the data were excluded from analyses. The EUS-EMG activity was passed through a discriminator, and the output was recorded with an amplifier and data-acquisition software (sampling rate 400 Hz; Chart, AD Instruments, Colorado Springs, CO) on a computer system equipped with an analog-to-digital converter (PowerLab, AD Instruments). The animals were placed in restraining cages as described above, and simultaneous measurements of intravesical pressure and EUS-EMG activity under an awake condition were performed during intravesical saline infusion after the recovery from anesthesia. After rhythmic bladder contractions and EUS-EMG activities were confirmed for at least 60 minutes, two serial filling CMGs and EUS-EMGs were recorded and then averaged for statistical analyses. CMG-EMG traces during the voiding phase can detect intermittent voiding coinciding with reductions in intravesical pressure in CMG recordings, which occurred during periods of reduced EUS-EMG activity (Figure 2). In CMG-EMG recordings, we measured voiding contraction time, duration of reduced EMG activity and the ratio of reduced EMG activity time to voiding contraction time. “Reduced” EMG activity was measured when EMG activity was reduced to the baseline level between tonic firings of EUS-EMG activity during voiding bladder contraction. The voiding contraction time was measured as a duration between the rise of intravesical pressure beyond the threshold pressure and the point at which intravesical pressure returned to the level of threshold pressure. These EUS-EMG parameters were obtained during the voiding phase of at least two voiding cycles and averaged for statistical comparison.

2.4 | Real-time reverse-transcription polymerase chain reaction

L6 DRG were removed bilaterally in a separate group of CSF-treated SCI mice ($n = 8$) and p38 MAPK inhibitor-treated SCI mice ($n = 5$) as well as CSF-treated SI mice ($n = 6$). We added an SI group for this molecular study, but not functional CMG-EMG studies, because we have previously reported the urodynamic comparison data between SI and SCI mice.¹⁰ These specimens were immediately frozen in liquid nitrogen and stored at -80°C until further processing. Real-time PCR was performed using the MX3000P system (Stratagene, La Jolla, CA). The primers sequences used were as follows: Actb (NM_007393.5; forward primer, GCCCTGAGGCTCTTTTCCAG; reverse primer, TGCCACAGGATTCCAT ACCC), TRPV1 (NM_001001445.2; forward primer, TACTTTTCTTTGTACAGTCACT; reverse primer, TCAATCATGACAGCATAGAT); TNF- α (NM_013693.3; forward primer, AGCCGATTTGCTATCTCATA CCAG; reverse primer, CCTTCACAGAGCAA TGACTION); and iNOS (NM_010927.4; forward primer, GGGCAGCCTGTGAGACCTT; reverse primer, TGAGGGCTCTGTTGAGGTCTA). The cycle conditions comprised a 10-minute polymerase activation and 40 cycles of denaturation at 95°C for 15 seconds, annealing at 55°C for 30 seconds, and extension at 72°C for 30 seconds followed by dissociation from 55°C to 95°C . The reactions were performed in triplicate and the relative quantities of messenger RNA (mRNA) were normalized to the house keeping control gene β -actin (Actb). Real-time PCR data were analyzed by the DCp (difference in crossing points) method as $R = 2^{(Cp \text{ sample} - Cp \text{ control})}$ to generate the relative expression ratio (R) of each target gene relative to that of Actb. We also determined the specificity of the

complementary DNA using real-time PCR to verify that our primer/probe sets did not amplify genomic DNA.

2.5 | Statistical analysis

Results are reported as the mean \pm standard error. One-way analysis of variance with post hoc Mann-Whitney *U* test was used to calculate the statistical significance among the groups.

2.6 | Ethical approval

All animal experiments were conducted in accordance with the ARRIVE and National Institutes of Health guidelines and approved by the Institutional Animal Care and Use Committees (IACUC) (Protocol approval #15,086,776).

3 | RESULTS

3.1 | CMG recordings

In p38 MAPK inhibitor-treated SCI mice, single CMG recordings revealed that NVCs during bladder filling were significantly reduced (Figure 1), VV and voiding efficiency were significantly improved, and MP was significantly increased compared with measurements in CSF-treated SCI mice (Figure 1 and Table 1). In addition, bladder capacity was significantly smaller in p38 MAPK inhibitor-treated SCI mice than in CSF-treated SCI mice (Table 1).

3.2 | Simultaneous CMG and EUS-EMG recordings

Because we found an improvement of voiding dysfunction evident as increased VV and voiding efficiency in SCI mice after p38 MAPK inhibitor treatment in CMG, the subsequent simultaneous CMG and EUS-EMG recordings were performed to elucidate the effects of a p38 MAPK inhibitor on DSD in SCI mice. We found that there was no significant difference in the duration of reduced EMG activity time or voiding contraction time during the voiding phase between p38 MAPK inhibitor-treated and CSF-treated SCI mice (Figure 1 and Table 1), indicating that p38 MAPK inhibitor treatment did not improve DSD in SCI. All mice were confirmed to be implanted with electrodes within 1 mm of the urethra after experiments.

3.3 | Real-time reverse-transcription polymerase chain reaction

The expression levels of transient receptor potential cation channel subfamily V member 1 (TRPV1), tumor necrosis factor- α (TNF- α), and inducible nitric oxide synthase (iNOS) mRNA were increased in SCI mice compared with measurements in SI mice. The levels in SCI mice were significantly decreased after p38 MAPK inhibitor treatment (Figure 3).

4 | DISCUSSION

The present study revealed that intrathecal treatment of SCI mice with a p38 MAPK inhibitor: (a) reduced NVCs, a CMG parameter that reflects DO, (b) improved voiding efficiency, (c) decreased TRPV1, TNF- α , and iNOS mRNA levels in L6 DRG, all of which were increased after SCI. However the inhibitor did not alter EUS-EMG parameters. These

results raise the possibility that signaling molecules acting via intracellular p38 MAPK mechanisms contribute to some of the neurogenic LUTD produced by SCI.

It is known that p38 MAPK in DRG and in the spinal cord is activated by injury to peripheral nerves or the spinal cord and that neurotrophins such as NGF play a role in this activation. Neurotrophins are considered to be important factors in various types of neural plasticity that underlies the recovery of bladder function and the emergence of LUTD after SCI in rats and mice.^{5,7,11,12} Previous studies using SCI rats and mice also demonstrated that overdilatation of the bladder increases NGF production in the bladder, which could enhance C-fiber afferent nerve excitability, leading to neurogenic DO after SCI.^{3-5,7} Vizzard et al showed that the immunoreactivity of TrkA, which is a high-affinity receptor for NGF, is predominantly expressed in C-fiber afferent neurons and is increased in rat bladder afferent neurons after SCI.^{13,14} We recently reported that anti-NGF antibody treatment in SCI mice reduced C-fiber-dependent NVCs during bladder filling and reduced hyperexcitability of TRPV1 positive, capsaicin-sensitive C-fiber bladder afferent neurons.^{5,15,16} It has also been reported that NGF-activation of p38 MAPK increases the expression of TRPV1 receptor in DRG neurons.⁸ Therefore, it is likely that p38 MAPK activation in bladder afferent pathways after SCI contributes to C-fiber afferent hyperexcitability at least in part via upregulation of TRPV1, leading to NVCs during the storage phase.

Phosphorylated p38 MAPK is expressed primarily in small- to medium-sized DRG neurons, which are the same types of A δ and C-fiber afferent neurons that innervate the bladder.¹⁷ A recent study using a novel herpes simplex virus vector-mediated neuronal labeling technique indicated that SCI in mice induces an expansion of the TRPV1-expressing C-fiber afferent population and that the average cell size of TRPV1-expressing cells is decreased after SCI.¹⁸ These results suggest that SCI induces de novo expression of TRPV1 in small-sized C-fiber bladder afferent neurons, thereby increasing afferent excitability. Thus, NGF-induced phosphorylation of p38MPAK may contribute to TRPV1 overexpression in small-sized, C-fiber bladder afferent neurons after SCI¹⁸ although further studies are needed to investigate the effects of p38 inhibition on total and phosphorylated levels of p38 MAPK expression as well as subpopulation-specific changes in TRPV1 expression in bladder afferent pathways.

Several observations indicate that signaling molecules in addition to NGF are involved in the p38 MAPK-induced plasticity of afferent neurons and bladder function after SCI in mice. Firstly, mRNA levels of TRPV1 in L6 DRGs were increased after SCI and reduced by p38 MAPK inhibition (Figure 3); while NGF is known to increase TRPV1 expression in DRGs in a transcription- independent manner.⁸ Furthermore, in the current study, intrathecal p38 MAPK inhibitor treatment not only reduced DO, but also improved voiding in SCI mice, while our previous study showed that anti-NGF antibody treatment reduced DO during bladder filling without affecting voiding efficiency in SCI mice.⁵

The improvement in voiding after p38 MAPK inhibition was also associated with increased maximal bladder pressures during voiding, while anti-NGF treatment did not change MP,⁵ providing further evidence that some of p38 MAPK effects on voiding are mediated by mechanisms unrelated to NGF. The difference in the afferent mechanisms triggering DO and voiding is also evident in the differential sensitivity to capsaicin-induced C-fiber

desensitization in SCI rodent models, in which capsaicin blocks DO, but not voiding contractions.^{15,19} These observations suggest that voiding is induced by activation of A δ -fiber bladder afferents rather than capsaicin-sensitive C-fiber afferents. Our finding in this study showing a reduction in bladder capacity, at which the A δ -fiber-dependent voiding reflex is induced, after p38 MAPK inhibition also supports this assumption that A δ -fiber bladder afferent function is enhanced after p38 MAPK inhibitor treatment. However, the existence of capsaicin-insensitive, C-fiber bladder afferent neurons^{20,21} raises the possibility that a second population of C-fiber afferents may also contribute to voiding after SCI and that inhibition of P38 MAPK in these afferents could enhance the A δ -fiber-mediated bladder micturition contractions to improve voiding. Further studies are anticipated to clarify the underlying mechanisms of P38 MAPK-mediated modulation of A δ -fiber-dependent voiding function in SCI.

Various studies have demonstrated that spinal p38 MAPK inhibition reduces inflammation and neuropathic pain in animal models.^{22–24} In this study, mRNA levels of two inflammatory mediators, TNF- α and iNOS, were increased in L6 DRG after SCI and significantly decreased after p38 MAPK inhibitor treatment in SCI mice, suggesting that inflammatory mechanisms in bladder afferent pathways mediated by the p38 MAPK signaling may also contribute to storage and voiding dysfunctions after SCI.

In this study, intrathecal administration was used as an experimental method to confirm that p38 MAPK activation in afferent pathways or in the spinal cord, but not in the bladder, play an important role in SCI-induced LUTD. Our findings support the idea that neuronal p38 MAPK is an important signaling molecule to induce SCI-induced LUTD, although when considering the clinical translation of this study, more experiments are needed to clarify whether systemic application of p38 MAPK inhibitors is similarly effective in reducing LUTD after SCI. Also, a limitation of the present study is that a group of SI mice treated with a p38 MAPK inhibitor was not included. Because there may be the possibility that the p38 MAPK inhibitor treatment increases maximum MP and decreases bladder capacity in SI mice, as shown in SCI mice, a further study using SI animals needs to be performed.

5 | CONCLUSIONS

In SCI mice, inhibition of p38 MAPK reduced DO evident as reduced NVCs, and improved voiding evident as increased VV and MP during the voiding phase, although it did not affect DSD during voiding bladder contractions. These results suggest that p38 MAPK signaling pathways may play an important role, at least in part, as a downstream mechanism activated by NGF, in the emergence of LUTD after SCI.

ACKNOWLEDGMENTS

This study was supported by grants from NIH (NIH P01 DK093424), DOD (W81XWH-17-1-0403), and KAKENHI for Early-Career Scientists (18K16751).

Funding information

U.S. Department of Defense, Grant/ Award Number: W81XWH-17-1-0403; KAKENHI, Grant/Award Number: 18K16751; Foundation for the National Institutes of Health, Grant/Award Number: NIH P01 DK093424

REFERENCES

1. de Groat WC, Yoshimura N. Plasticity in reflex pathways to the lower urinary tract following spinal cord injury. *Exp Neurol*. 2012;235:123–132. [PubMed: 21596038]
2. de Groat WC, Griffiths D, Yoshimura N. Neural control of the lower urinary tract. *Compr Physiol*. 2015;5:327–396. [PubMed: 25589273]
3. Seki S, Sasaki K, Fraser MO, et al. Immunoneutralization of nerve growth factor in lumbosacral spinal cord reduces bladder hyperreflexia in spinal cord injured rats. *J Urol*. 2002;168:2269–2274. [PubMed: 12394773]
4. Seki S, Sasaki K, Igawa Y, et al. Suppression of detrusor-sphincter dyssynergia by immunoneutralization of nerve growth factor in lumbosacral spinal cord in spinal cord injured rats. *J Urol*. 2004;171:478–482. [PubMed: 14665959]
5. Wada N, Shimizu T, Shimizu N, et al. The effect of neutralization of nerve growth factor (NGF) on bladder and urethral dysfunction in mice with spinal cord injury. *NeuroUrol Urodyn*. 2018;37:1889–1896. [PubMed: 29516546]
6. Elg S, Marmigere F, Mattsson JP, Ernfors P. Cellular subtype distribution and developmental regulation of TRPC channel members in the mouse dorsal root ganglion. *J Comp Neurol*. 2007;503:35–46. [PubMed: 17480026]
7. Yoshimura N, Bennett NE, Hayashi Y, et al. Bladder overactivity and hyperexcitability of bladder afferent neurons after intrathecal delivery of nerve growth factor in rats. *J Neurosci*. 2006;26:10847–10855. [PubMed: 17050722]
8. Ji RR, Samad TA, Jin SX, Schmolli R, Woolf CJ. p38 MAPK activation by NGF in primary sensory neurons after inflammation increases TRPV1 levels and maintains heat hyperalgesia. *Neuron*. 2002;36(1):57–68. [PubMed: 12367506]
9. Cuenda A, Rousseau S. p38 MAP-kinases pathway regulation, function and role in human diseases. *Biochim Biophys Acta*. 2007;1773:1358–1375. [PubMed: 17481747]
10. Kadekawa K, Yoshimura N, Majima T, et al. Characterization of bladder and external urethral activity in mice with or without spinal cord injury—a comparison study with rats. *Am J Physiol Regul Integr Comp Physiol*. 2016;310:R752–R758. [PubMed: 26818058]
11. Keefe K, Sheikh I, Smith G. Targeting neurotrophins to specific populations of neurons: NGF, BDNF, and NT-3 and their relevance for treatment of spinal cord injury. *Int J Mol Sci*. 2017;18:548.
12. Vizzard MA. Neurochemical plasticity and the role of neurotrophic factors in bladder reflex pathways after spinal cord injury. *Prog Brain Res*. 2006;152:97–115. [PubMed: 16198696]
13. Qiao L, Vizzard MA. Upregulation of tyrosine kinase (Trka, Trkb) receptor expression and phosphorylation in lumbosacral dorsal root ganglia after chronic spinal cord (T8-T10) injury. *J Comp Neurol*. 2002;449:217–230. [PubMed: 12115676]
14. Vizzard MA. Changes in urinary bladder neurotrophic factor mRNA and NGF protein following urinary bladder dysfunction. *Exper Neurol*. 2000;161:273–284. [PubMed: 10683293]
15. Kadekawa K, Majima T, Shimizu T, et al. The role of capsaicin-sensitive C-fiber afferent pathways in the control of micturition in spinal-intact and spinal cord-injured mice. *Am J Physiol Renal Physiol*. 2017;313:F796–F804. [PubMed: 28637786]
16. Shimizu T, Majima T, Suzuki T, et al. Nerve growth factor-dependent hyperexcitability of capsaicin-sensitive bladder afferent neurones in mice with spinal cord injury. *Exp Physiol*. 2018;103:896–904. [PubMed: 29603450]
17. Cheng HT, Dauch JR, Oh SS, et al. p38 mediates mechanical allodynia in a mouse model of type 2 diabetes. *Mol Pain*. 2010;6:28. [PubMed: 20482876]
18. Shimizu N, Doyal MF, Goins WF, et al. Morphological changes in different populations of bladder afferent neurons detected by herpes simplex virus (HSV) vectors with cell-type-specific promoters in mice with spinal cord injury. *Neuroscience*. 2017;364:190–201. [PubMed: 28942324]
19. Cheng CL, Ma CP, de Groat WC. Effect of capsaicin on micturition and associated reflexes in chronic spinal rats. *Brain Res*. 1995;678:40–48. [PubMed: 7620897]

20. Yoshimura N, Erdman SL, Snider MW, de Groat WC. Effects of spinal cord injury on neurofilament immunoreactivity and capsaicin sensitivity in rat dorsal root ganglion neurons innervating the urinary bladder. *Neuroscience*. 1998;83:633–643. [PubMed: 9460769]
21. Yoshimura N, Seki S, Erickson KA, Erickson VL, Chancellor MB, Groat WC. Histological and electrical properties of rat dorsal root ganglion neurons innervating the lower urinary tract. *J Neurosci*. 2003;23:4355–4361. [PubMed: 12764124]
22. Horiuchi H, Ogata T, Morino T, Chuai M, Yamamoto H. Continuous intrathecal infusion of SB203580, a selective inhibitor of p38 mitogen-activated protein kinase, reduces the damage of hind-limb function after thoracic spinal cord injury in rat. *Neurosci Res*. 2003;47:209–217. [PubMed: 14512145]
23. Qu WS, Tian DS, Guo ZB, et al. Inhibition of EGFR/MAPK signaling reduces microglial inflammatory response and the associated secondary damage in rats after spinal cord injury. *J Neuroinflammation*. 2012;9:178. [PubMed: 22824323]
24. Taves S, Berta T, Liu DL, et al. Spinal inhibition of p38 MAP kinase reduces inflammatory and neuropathic pain in male but not female mice: sex-dependent microglial signaling in the spinal cord. *Brain Behav Immun*. 2016;55:70–81. [PubMed: 26472019]

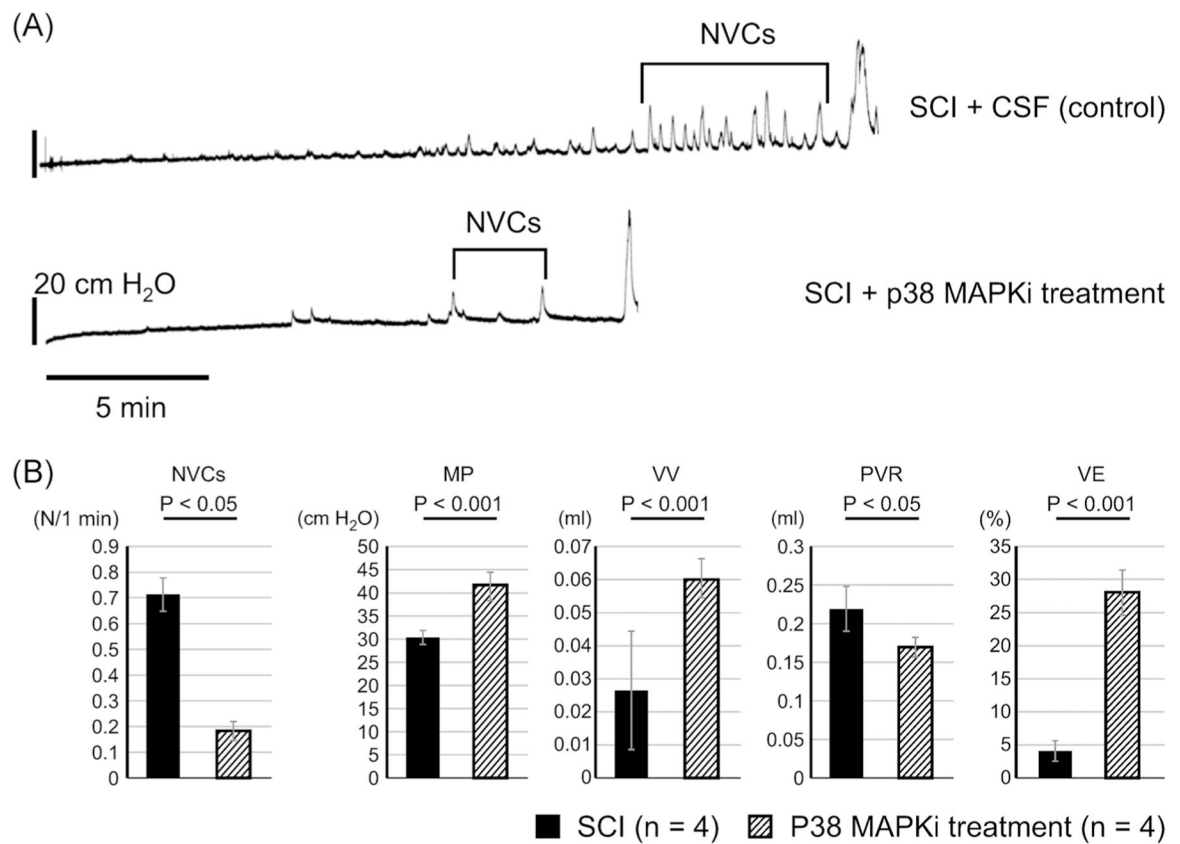
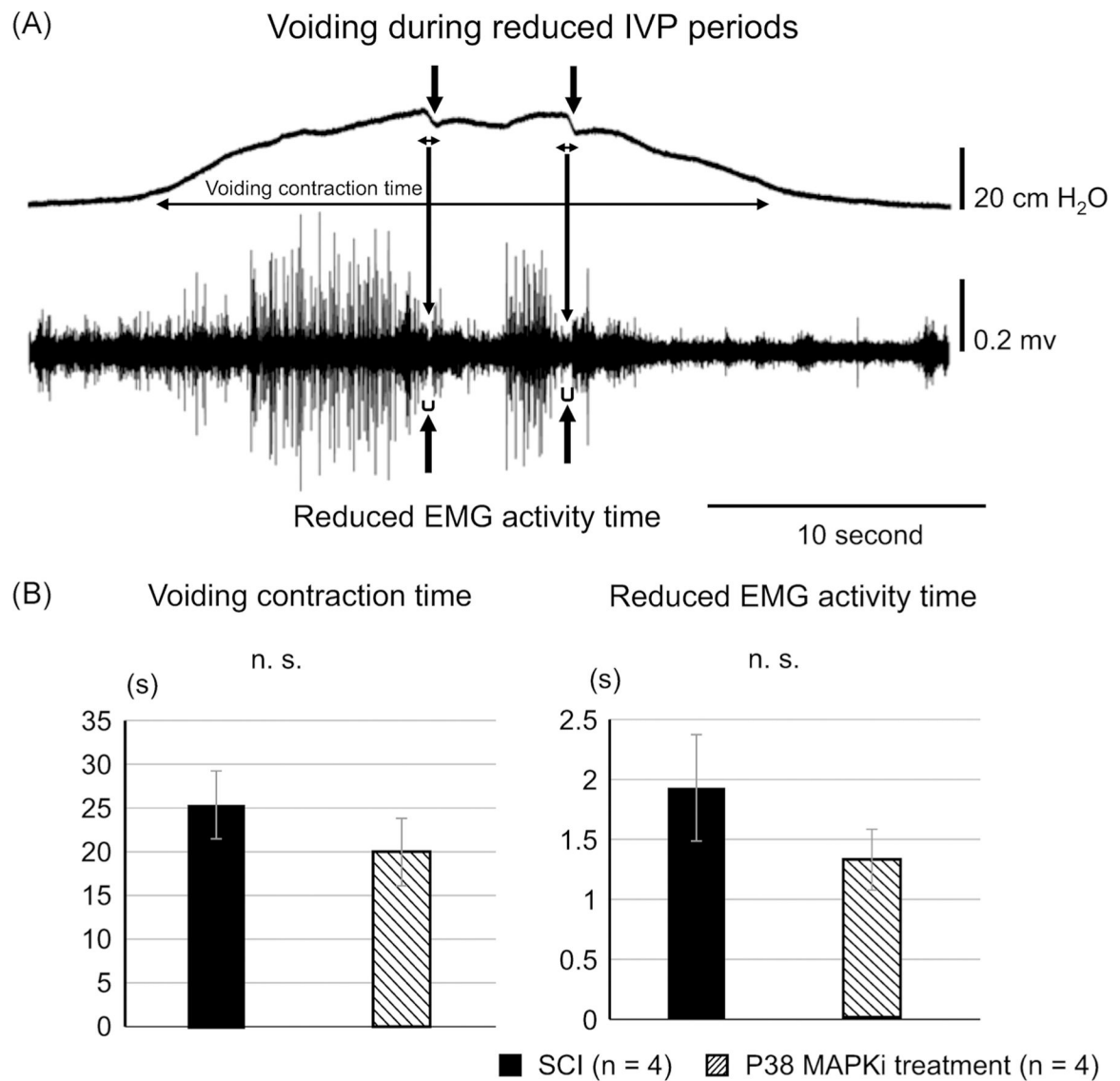


FIGURE 1.

A, Representative CMGs in SCI mice with CSF or p38 MAPKi treatment. The number of NVCs was reduced in p38 MAPK inhibitor-treated SCI mice. B, CMG parameters in SCI mice treated intrathecally with CSF or p38 treatment. VE was significantly improved as shown by increases in VV and MP, and a decrease in PVR in p38 MAPK inhibitor-treated SCI mice (P38 treatment) compared with CSF-treated SCI mice. CMG, cystometrogram; CSF, cerebrospinal fluid; MAPK, mitogen-activated protein kinase; MP, micturition pressure; NVC, nonvoiding contraction; p38 MAPKi, p38 MAPK inhibitor; PVR, post-void residual volume; SCI, spinal cord injury; VE, voiding efficiency; VV, voided volume

**FIGURE 2.**

A, Representative CMG and EUS-EMG recordings. CMG-EMG traces during the voiding phase can detect intermittent voiding coincided with notch-like reductions in intravesical pressure (\downarrow) in the CMG recording (upper trace), which occurred during periods of reduced EUS-EMG activity (\uparrow). Actual voids occur during these reduced EUS-EMG periods. Voiding contraction time, reduced EMG activity duration, and the ratio of reduced EMG activity time to voiding contraction time were measured in SCI mice with or without p38 MAPK inhibitor treatment. B, CMG-EMG parameters during voiding. The voiding contraction time and the reduced EMG activity time during the voiding phase were not significantly different (n.s.) between p38 MAPK inhibitor-treated (P38 treatment) and CSF-treated SCI mice. CMG, cystometrogram; CSF, cerebrospinal fluid; EMG, electromyogram; EUS, external urethral sphincter; IVP, intravesical pressure; MAPK, mitogen-activated protein kinase; SCI, spinal cord injury

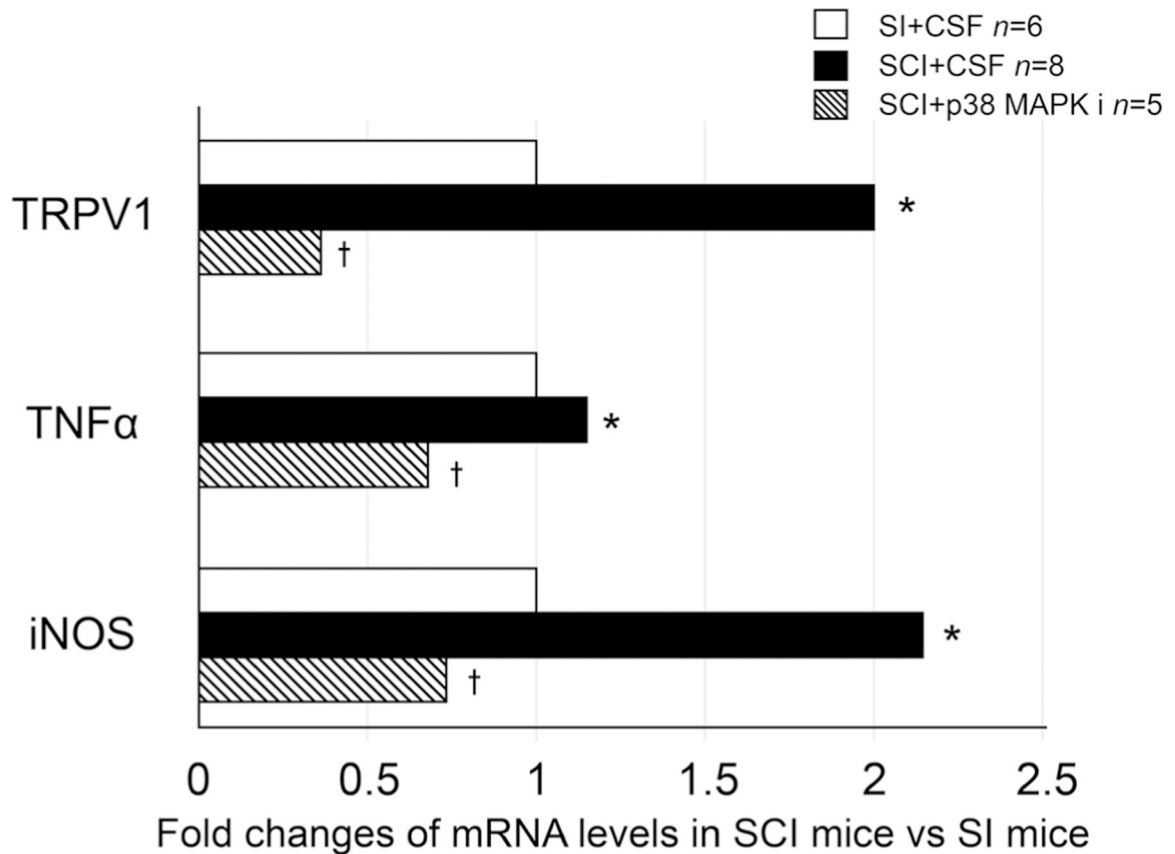


FIGURE 3.

mRNA levels of TRPV1, TNF- α , and iNOS of L6 DRG. In SCI mice, TRPV1, TNF- α , and iNOS levels were higher than those of SI mice with CSF treatment. After p38 MAPKi treatment, TRPV1, TNF- α , and iNOS levels in SCI mice were lower than those of SCI mice with CSF treatment. Data are shown as relative values of mRNA expression in SCI mice vs SI mice whereas the statistical analysis was performed using the mRNA expression ratio against the house keeping gene (β -actin) calculated in each mouse. * $P < .05$ vs SI+CSF mice. † $P < .05$ vs SCI + CSF mice. CSF, cerebrospinal fluid; DRG, dorsal root ganglia; iNOS, inducible nitric oxide synthase; mRNA, messenger RNA; p38 MAPKi, p38 MAPK inhibitor; SI, spinal intact; SCI, spinal cord injury; TNF- α , tumor necrosis factor- α ; TRPV1, transient receptor potential cation channel subfamily V member 1

TABLE 1
CMG and CMG-EMG parameters in SCI mice with CSF or p38 MAPK inhibitor treatment

	SCI mice with CSF	SCI mice with p38 MAPKi
Cystometry parameters		
Number of animals	4	4
Number of NVCs/1 min	0.71 ± 0.06	0.18 ± 0.03 *
Micturition pressure, cmH ₂ O	30.33 ± 1.5	41.4 ± 2.9 *
Voided volume, mL	0.026 ± 0.018	0.06 ± 0.006 *
Post-void residual, mL	0.22 ± 0.028	0.17 ± 0.014 *
Voiding efficiency, %	4 ± 1.6	29 ± 3.4 *
Cystometry-electromyogram parameters		
Voiding contraction time, s	25.4 ± 3.7	19.8 ± 3.8
Reduced EMG activity time, s	1.44 ± 0.43	0.91 ± 0.26

Abbreviations: CMG, cystometrogram; CSF, cerebrospinal fluid; EMG, electromyogram; NVC, nonvoiding contraction; p38 MAPKi, p38 MAPK inhibitor; SCI, spinal cord injury.

* < .05 vs SCI mice with CSF.